A Mathematical Approach to the Mechanical Capabilities of Limbs and Fingers

Francisco J. Valero-Cuevas

Abstract Neuromuscular function is the interaction between the nervous system and the physical world. Limbs and fingers are, therefore, the ultimate mechanical filters between the motor commands that the nervous system issues and the physical actions that result. In this chapter we present a mathematical approach to understanding how their anatomy (i.e., physical structure) defines their mechanical capabilities. We call them "mechanical filters" because they attenuate, amplify, and transform neural signals into mechanical output. We explicitly distinguish between limbs and fingers because their subtle anatomical differences have profound effects on their mechanical properties. Our main message is that many aspects of neuromuscular function such as co-contraction, posture selection, muscle redundancy, optimality of motor command, are fundamentally affected (if not defined) by the physical structure of limbs and fingers. We attempt to present the fundamental filtering properties of limbs and fingers in a unified manner to allow for a direct and useful application of powerful mathematical concepts to the study of neuromuscular function. Every researcher of motor control is well advised to consider these filtering properties to properly understand the co-evolution and synergistic interactions between brain and body. At the end of the day, every inquiry in neuromuscular function can be reduced to the fundamental question whether and how the nervous system can perform the necessary sensorimotor functions to exploit and reach the mechanical capabilities of limbs and fingers.

F.J. Valero-Cuevas (✉)
Department of Biomedical Engineering, The University of Southern California,
3710 McClintock Ave, Los Angeles, CA 90089-2905, USA
e-mail: valero@USC.edu

D. Sternad (ed.), *Progress in Motor Control*,
DOI 10.1007/978-0-387-77064-2_33,

Limbs and Fingers Transform the Output of the Nervous System into Mechanical Actions

The anatomical structure of limbs and fingers takes as inputs muscular actions and produces as outputs motions and forces. We will use the generic term "limb" for both limbs and fingers, and will distinguish between them where necessary. We begin by applying the mathematical tools of robotics where the limb is a serial kinematic chain of rigid links articulated by rotational joints, and muscles are idealized as linear actuators that produce joint torques (for a more detailed discussion see (Yoshikawa, 1990; Valero-Cuevas et al., 1998)). The propagation of information and/or energy through the system can be described as a forward model or, alternatively, as a serial cascade of filters (Fig. 1). In this chapter we call the neuromuscular system a series of "mechanical filters" because they attenuate, amplify, and transform neural signals into mechanical output.

To analyze the idealized 3-joint limb shown in Fig. 2, the first step in defining the mapping from muscular actions to mechanical outputs is to establish the mapping from joint angles (the vector of three generalized rotational coordinates $\vec{q} = \{q_1, q_2, q_3\}^T$) to limb endpoint position and orientation (the vector of three endpoint coordinates $\vec{x} = \{x, y, \alpha\}^T$) for a given set of link lengths:

$$\begin{aligned} \vec{x} = G(\vec{q}) &= \left\{ \begin{array}{c} G_x(\vec{q}) \\ G_y(\vec{q}) \\ G_\alpha(\vec{q}) \end{array} \right\} \\ &= \left\{ \begin{array}{c} L_1 \cos(q_1) + L_2 \cos(q_1 + q_2) + L_3 \cos(q_1 + q_2 + q_3) \\ L_1 \sin(q_1) + L_2 \sin(q_1 + q_2) + L_3 \sin(q_1 + q_2 + q_3) \\ q_1 + q_2 + q_3 \end{array} \right\} \end{aligned} \tag{1}$$

where $G(\vec{q})$ is the geometric model defined by the trigonometric equations for the end point position $\{x, y\}^T$ and orientation $\{\alpha\}$ of the last link as a function

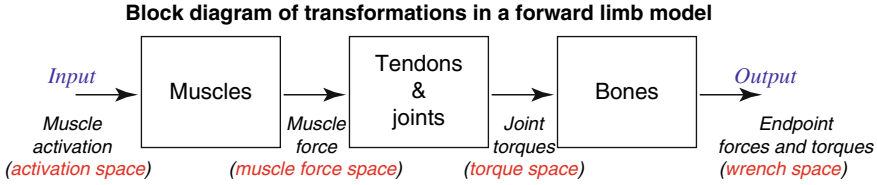

Fig. 1 The production of mechanical function by limbs and fingers is the consequence of a sequence of transformations from muscle activation to muscle force, to joint torques, and finally to endpoint accelerations and force and toques. The figure illustrates a static case, where the output of the limb end point is a wrench (the vector of forces and torques) resisted by the environment

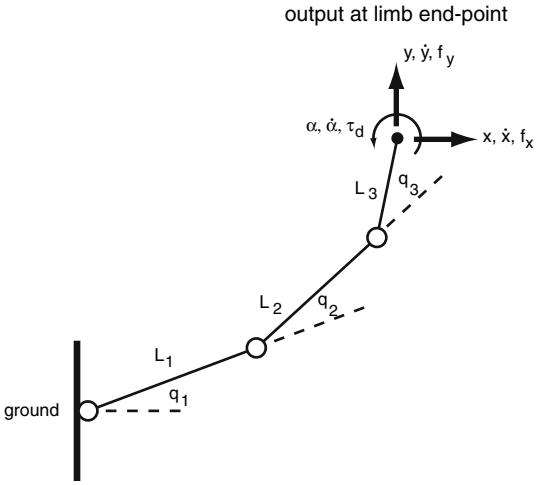

Fig. 2 A limb with three rotational joints has three rotational DOFs ($\vec{q} = \{q_1, q_2, q_3\}^T$) and three end point DOFs ($\vec{x} = \{x, y, \alpha\}^T$). The rotational kinetic inputs are three net joint torques ($\vec{\tau} = \{\tau_1, \tau_2, \tau_3\}^T$) that produce the output wrench vector ($\vec{w} = \{f_x, f_y, \tau_d\}^T$). These transformations are governed by equations 1–4

of $\vec{q}$ and link lengths L. The second step is to define the transformation from joint angular velocities ($\dot{\vec{q}} = \{\dot{q}_1, \dot{q}_2, \dot{q}_3\}^T$, the time derivative of $\vec{q}$) to limb endpoint velocities ($\dot{\vec{x}} = \{\dot{x}, \dot{y}, \dot{\alpha}\}^T$, the time derivative of $\vec{x}$):

$$\dot{\vec{x}} = J(\vec{q})\dot{\vec{q}} = \begin{pmatrix} \frac{\partial G_x(\vec{q})}{\partial q_1} & \frac{\partial G_x(\vec{q})}{\partial q_2} & \frac{\partial G_x(\vec{q})}{\partial q_3} \\ \frac{\partial G_y(\vec{q})}{\partial q_1} & \frac{\partial G_y(\vec{q})}{\partial q_2} & \frac{\partial G_y(\vec{q})}{\partial q_3} \\ \frac{\partial G_\alpha(\vec{q})}{\partial q_1} & \frac{\partial G_\alpha(\vec{q})}{\partial q_2} & \frac{\partial G_\alpha(\vec{q})}{\partial q_3} \end{pmatrix} \dot{\vec{q}} \tag{2}$$

where $J(\vec{q})$ is the Jacobian of the partial derivatives of the geometric model of the limb with respect to $\dot{\vec{q}}$ (Yoshikawa, 1990). Writing equation 2 as $\dot{\vec{x}} = J\dot{\vec{q}}$ serves to highlight that the transformation from $\dot{\vec{q}}$ to $\dot{\vec{x}}$ is a linear mapping by the matrix J, which is constant for a given limb posture $\vec{q}$, but which changes in a nonlinear way with posture. Fig. 2 shows a sample planar limb with its geometric model and Jacobian in equations 1 and 2, respectively. Please note that the contents of the output vectors $\vec{x}$ and $\dot{\vec{x}}$ is mixed because they contain both translational and rotational kinematic information. Because the system has three degrees of freedom in the plane, the joints can control the position of the endpoint and the orientation of the last link (and their linear and angular velocities) (Yoshikawa, 1990; Valero-Cuevas et al., 1998).

The Jacobian in equation 2 also establishes the mapping from joint torques (the vector of three generalized net joint torques at each joint $\vec{\tau} = \{\tau_1, \tau_2, \tau_3\}^T$) to static limb endpoint forces and torques (the wrench $\vec{w} = \{f_x, f_y, \tau_d\}^T$) if motion or rotation of the endpoint is opposed:

$$\vec{w} = J(\vec{q})^{-T}\vec{\tau} \tag{3}$$

Once again, writing equation 3 as $\vec{w} = J^{-T}\vec{\tau}$ serves to highlight that the transformation from $\vec{\tau}$ to $\vec{w}$ is a linear mapping by the matrix J^{-T}, which is constant for a given limb posture $\vec{q}$, but changes in a nonlinear way as posture changes. Similarly, the mechanical output at the third link is a combination of endpoint forces $\{f_x, f_y\}^T$ and torque $\{\tau_d\}$ (Yoshikawa, 1990; Valero-Cuevas et al., 1998).

Torque Space Formulation

We can now investigate several concepts of neuromuscular control related to the mapping from net joint torques to endpoint wrenches (i.e., forces and torques). Consider that the magnitude of positive and negative torque at each joint can be represented as a number along a coordinate line, with the convention that flexion torques are positive and extension torques negative. Then the torque actuation of a 3-joint system, described in vector form as $\vec{\tau} \in^{\circ 3}$, can be visualized graphically as a point in 3-D "torque space." Moreover, whereas the torque space is the domain of J^{-T}, its codomain is the 3-D "wrench space" with dimensions f_x, f_y and τ_d that fully describes the static mechanical output of the endpoint of the limb if it is constrained.

Suppose now that the limb's musculature is capable of producing combinations of net joint torques that satisfy the equation:

$$|\vec{\tau}| = \sqrt{\tau_1^2 + \tau_2^2 + \tau_3^2} = 1 \tag{4}$$

That is, every possible input vector $\vec{\tau}$ (i.e., combination of net joint torques) is contained in and described by the unit sphere (for a more detailed description of this analysis see (Yoshikawa, 1990)). Fig. 3 shows how the singular value decomposition of J^{-T} allows us to calculate the manipulating force ellipsoids for the limb, which quantify how the relative link lengths and joint angles affect the transformation of input joint torques into output wrenches. Briefly, at a given posture and for a constant magnitude of input torque, the limb will produce relatively larger or smaller output wrenches. More formally:

$$\sigma_1 \geq |\vec{w}| = \left|J^{-T}\vec{\tau}\right| \geq \sigma_3, \forall |\vec{\tau}| = 1 \tag{5}$$

where σ_1 and σ_3 are the largest and smallest singular values of J^{-T}, respectively. equation 5 shows how, like a filter, the limb has an intrinsic maximal and minimal "mechanical gain" in specific directions of the wrench space. Shown graphically in Fig. 3, we see that J^{-T}distorts the unit sphere of the input torque into an ellipsoid describing the wrench output. The semi-major and semi-minor axes of the ellipse in the wrench space have lengths $2^*\sigma_1$ and $2^*\sigma_3$, respectively, and whose orientation is given by the left singular vectors of J^{-T}.

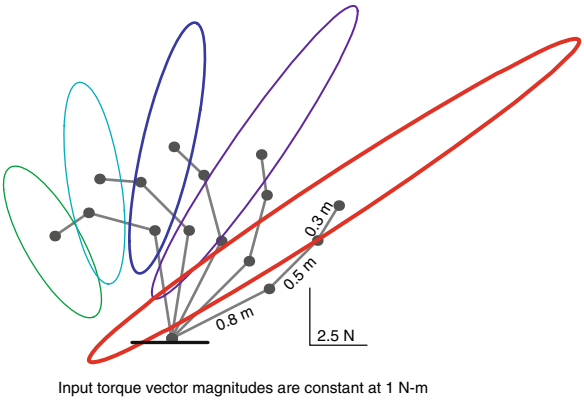

Fig. 3 The mechanical structure of the system defines the input-output gain from net joint torques to endpoint wrenches. For example, the manipulating force ellipsoids indicate how there are directions in which the endpoint forces are more or less easily produced for a same magnitude of input (in this case, a unit vector of net joint torques (equation 4). Note how dramatically the size, shape and orientation of these preferred directions changes with posture. This 2D plot of the transformation described in equation 3 shows only the output forces (f_x,f_y), where the magnitude of the output torque at the last link (τ_d) is not shown for clarity

Importantly, the same analysis can be carried out with J, whose 3-D domain and 3-D codomain are the input angular velocity space ($\dot{\vec{q}}$) and output endpoint velocity space ($\dot{\vec{x}}$), respectively. In this case, a unit input sphere of angular velocities is mapped into a manipulability ellipsoid whose size, shape and orientation are affected by the posture of the limb and its relative link lengths.

Consequences to Neuromuscular Control: Manipulability and Manipulating Force Ellipsoids

The manipulability and manipulating force ellipsoids clearly show that the geometric makeup of the limb is a critical filter of muscle actuation, independently of the coordination strategy used. By quantifying how the posture of the limb and the relative lengths of the links affect its mechanical filtering, one can begin to understand the evolutionary pressures on limb geometry for different tasks (e.g., limbs used for galloping vs. those used for digging), and the choice of limb posture for specific tasks (e.g., arm postures for hitting vs. writing). That is, because the manipulating force and manipulability ellipsoids can have vastly different aspect ratios depending on limb posture, some postures are better for tasks where similar force/velocity capabilities are needed in every direction (e.g., stirring a pot while holding a spoon with the elbow at 90° flexion) vs. postures for resisting high loads in specific directions (e.g., straighter limbs for standing), as shown in Fig. 3.

In the literature, the mapping from joint torques to endpoint velocities and forces is most often modeled as an over-constrained system where the assumed number of joints is fewer than six (the number of degrees of freedom of a rigid body). This allows exact solutions to torque time histories if the full kinematics and kinetics of the limb are known (Winter, 1990).

Muscle Space Formulation

Moving upstream along the chain of neuromuscular events (Fig. 1), we now focus on the under-constrained transformation from linear muscle forces into net joint torques. Consider that the magnitude of positive force produced by each independently controlled muscle (muscles can only pull, not push) is represented as a number along a coordinate line. Then the muscle actuation of, say, a 7-muscle system, described in vector form as $\vec{f} \in^{\circ 7}$, can be visualized graphically as a point in the positive quadrant of 7-D "muscle space" (Fig. 4 shows a 2 DOF limb with three muscles for ease of visualization). The transformation from positive muscle force, $\vec{f} = \{f_1, f_2, f_3, f_4, f_5, f_6, f_7\}^T$, to the lower-dimensional net joint torques at three joints, $\vec{\tau} = \{\tau_1, \tau_2, \tau_3\}^T$, is:

$$\vec{\tau} = R(\vec{q})\vec{f} = \begin{pmatrix} r_{11} & \cdots & r_{17} \\ \vdots & \ddots & \vdots \\ r_{31} & \cdots & r_{37} \end{pmatrix} \vec{f} \tag{6}$$

where $R(\vec{q})$ is the 3×7 matrix of moment arms (Valero-Cuevas et al., 1998), where each entry is the signed scalar moment arm value that transforms a positive muscle force into torques at the joints it crosses. Retaining our prior convention, positive moment arms signify that a flexion torque is produced by that muscle at that joint; the magnitude of the scalar is the distance from the line of action of the tendon path to the center of rotation of that joint. Moment arms often change as a function of posture due to tendon bowstringing and asymmetric bony geometry. This mapping by $R(\vec{q})$ from its domain (muscle space) to its lower-dimensional codomain (torque space) is the mathematical statement of the muscle "redundancy" that lies at the heart of much of motor control ("over-completeness" or "abundance" are also used in the literature).

A Mechanical Definition of Versatility: Spanning All Quadrants of the Output

Our goal is to present a mathematical perspective that is helpful in addressing the often misunderstood term of muscle redundancy. It is natural to begin by quoting the age-old question: "Why do we have so many muscles?" We prefer to ask it as: "How many muscles suffice for the endpoint of the limb to be

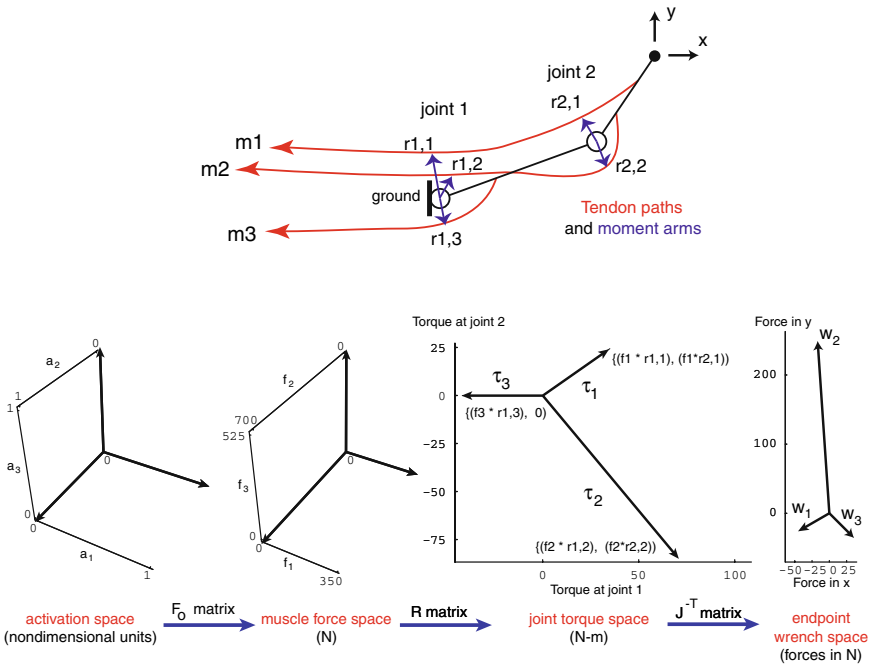

Fig. 4 Example of joint torque and endpoint force production for a 2-DOF, 3-muscle system. As shown in Fig. 1 and equation 7, the activations for each muscle can assume a value between 0 and 1 (activation space); which the F_0 matrix transforms into muscle forces between 0 and the maximal isometric force for that muscle (muscle force space; we ignore force-length and velocity properties for simplicity). The tendon routing defined in the R matrix maps muscle forces into joint torques (joint torque space). The Jacobian of the system transforms joint torques into endpoint wrenches (endpoint wrench space, in this case only x-y forces). Muscle coordination patterns can be interpreted as all possible vector additions of the 3 basis vectors in the activation, muscle force, joint torque and wrench spaces

versatile?"—and we provide examples of how it really depends on the mechanical task, as it has been appropriately pointed out by Loeb (Loeb, 2000).

We begin by defining biomechanical "versatility" and "feasibility." In this chapter, we propose the following working definition of biomechanical *versatility*: to be able to produce a wide variety of large net joint torques. Geometrically, this means to produce large magnitudes of net joint torques in *every direction* in torque space (Fig. 5) (Valero-Cuevas, 2005). This would enable the limb to produce static endpoint wrenches ($\vec{w}$) in every direction, as well as generate a wide variety of limb dynamics.[1] Regarding biomechanical feasibility,

[1] This is because a convex sets remains convex under linear mapping. Thus, if the musculature can produce net joint torques in every quadrant of the torque space, i.e., if its feasible torque set includes the origin, then the endpoint of the limb will also be able to produce wrenches (forces and torques) in every quadrant of the output wrench space. Its feasible wrench set will include the origin.

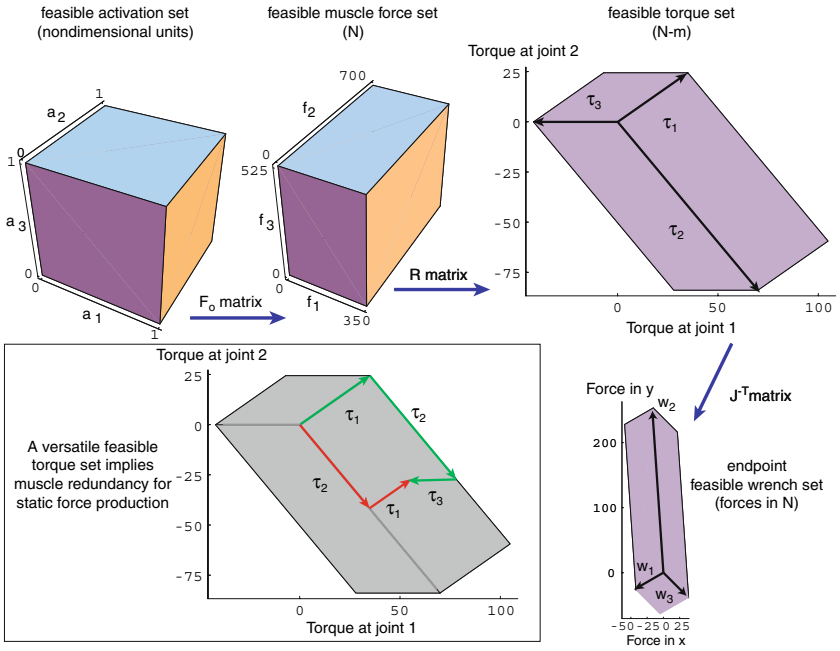

Fig. 5 Biomechanically feasible output of the limb in Figure 4. The family of all feasible activation patterns can be visualized as the feasible activation set (i.e., a cube in activation space whose dimensionality is equal to the number of muscles; in this case 3 for ease of visualization). The feasible activation set is then the set of all possible coordination patterns (i.e., points in the cube). Using the F_0 matrix, one finds the set of all possible muscle force combinations (the feasible muscle force set), which the R matrix maps into the feasible torque set, and J^{-T} maps into the feasible endpoint wrench space (which was defined as only forces for this 2-joint limb). The feasible torque and wrench sets are the range of all possible combinations of joint torques or endpoint forces, respectively, that the musculature is able to produce in that posture. Note that we present the concept that for a limb to be versatile, the feasible force set needs to include the origin to enable force production in every direction at the endpoint. Also note that *versatility unavoidably implies muscle redundancy* because including the origin necessarily leads to the geometric existence of multiple coordination patterns that can produce the same submaximal net joint torques (inset torque space) or endpoint wrenches

detailed discussions of the concept of feasible sets applied to biomechanics can be found in the literature (Kuo and Zajac, 1993; Valero-Cuevas et al., 1998; Valero-Cuevas, 2005). Briefly, any muscle coordination pattern (i.e., combination of muscle forces) is graphically described as a point in "muscle force space," which is the Cartesian space with as many orthogonal coordinates as there are muscles. Then, if each muscle can produce force from 0 to its maximal force, then the "feasible muscle force set" is the parallelepiped in the positive quadrant of muscle force space with dimensions given by the maximal force each muscle can produce. This volume fully describes all possible (i.e., feasible) muscle coordination patterns (Valero-Cuevas et al., 1998; Valero-Cuevas, 2000).

Consequences to Neuromuscular Control: The Feasible Torque Set

Thus the question of limb versatility can be posed mathematically as "For a given posture, does equation 6 transform the feasible muscle force set into a large feasible torque set that includes the origin?" The mapping in equation 6 is mediated by the routing of tendons. A common way to describe this graphically (Leijnse, 1996; Brand and Hollister, 1999; Valero-Cuevas, 2005) is to draw a vector for each muscle in torque space, where its components along each coordinate dimension are the magnitude of the torque produced by the muscle at that joint. That is, the slope of the vector is the ratio of moment arms across all joints crosses, and the magnitude of the vector is greatest for maximal muscle force (Fig. 4 and 5). The group of torque vectors from all muscles forms the "basis" in torque space, and all possible *positive* additions (Minkowski sum) of these vectors yield the "feasible torque set" which describes all possible net joint torques the musculature can produce (Valero-Cuevas, 2005) (Fig. 5).

The feasible torque set can be used to study the nature of "bi-" and "multi-articular" muscles. By the definition of biomechanical versatility above, a musculoskeletal system requires only $N+1$ *well-routed* muscles to produce feasible torque and wrench sets that include the origin (Valero-Cuevas, 2005). The geometric proof of this can be easily visualized in 2-D. Assume you have a system with 2 DOFs and uni-sense muscles (Fig. 6). We can easily use 2*N muscles for a limb with four mono-articular muscles. That is, an agonist-antagonist pair at each joint that have basis vectors along the coordinate axis to produce whose feasible torque set is a parallelogram that includes the origin. Similarly, we can have four muscles whose tendons are routed to produce two horizontal basis vectors (that actuate only the first DOF) plus two other diagonal basis vectors in the II and III quadrant produced by the bi-articular extensors and flexors, respectively (Fig. 6 left). This limb is also versatile because their positive linear combinations produce a feasible torque set in the shape of a parallelogram that includes the origin. Alternatively, we can design a versatile limb with only three (i.e., $N+1$) muscles, two of which have diagonal basis vectors in torque space (Fig. 6, right), because its feasible torque and wrench sets will also include the origin. Thus, by well-routed we mean that the anatomical routing of some muscles must cross more than one joint (a bi-articular muscle in this case) but also that some tendons should cross-over from being flexors to being extensors (as is the case of the extensor mechanism of the fingers, see below). The nature of these "bi-" and "multi-articular" muscles has been debated in the literature (Spoor, 1983), but this mechanical interpretation has been used to understand them. Thus the function of "bi-articular" muscles like the biceps femoris (hamstrings) or brachioradialis may have as much to do with the evolutionary pressure to create a large feasible torque set with few muscles as with the proposed neural control of multiple DOFs (Bobbert and van Ingen Schenau, 1988; van Ingen Schenau and Bobbert, 1993; van Soest et al., 1993).

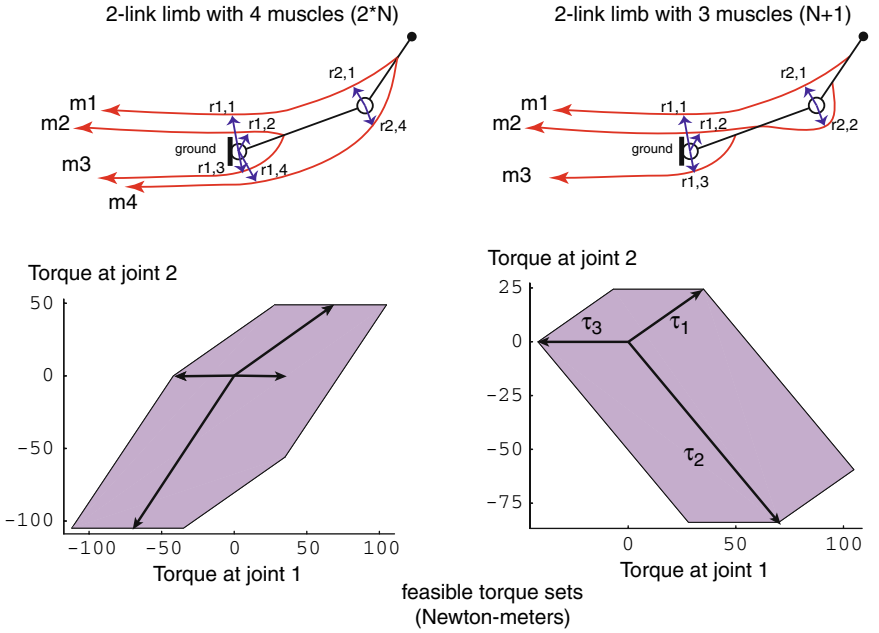

Fig. 6 For our definition of versatility, a system with 2 N muscles can be versatile, where N is the number of mechanical DOFs that the joints provide (*left*). However, N + 1 well routed muscles also suffice to create a versatile limb (*right*). Note that if we require that all muscles be located proximal to all joints (as is the case for fingers, but not of the limbs), cross-over tendons (m2 in the right figure, producing positive torque at one joint but negative torque at the other joint) are needed to create a versatile system by providing a diagonal basis vector in the 4th quadrant of the torque space (τ_2). τ_1 also provides a diagonal basis vector but, in contrast to τ_2, it produces positive torques at both joints it crosses. Such cross-over tendons as τ_2 are in fact found in the extensor mechanism of the fingers (Valero-Cuevas, 2005)

The anatomical peculiarity that fingers have muscles with tendons that "cross over" from being flexors to becoming extensors (the "extensor mechanism") can also be explained by this logic (Fig. 6) (Valero-Cuevas, 2005). Fingers have the anatomical constraint that their muscles are housed in the forearm and palm and are thus unable to have mono-articular muscles like larger limbs do. Therefore, all of their muscles are at least bi-articular, but mostly tri- and tetra-articular. This means that the basis vectors for the feasible torque set are all diagonal with respect to the coordinate axes. Muscles that run along the volar and dorsal aspects of the fingers are anatomically straightforward and exist as the flexor profundus or extensor digitorum groups, respectively. They have basis vectors in torque space that span the 1st and 3rd quadrants of a 2 DOF finger. Note that additional muscles with basis vectors directed down and to the right will dramatically increase torque production in the 4th quadrant, which we have found to be beneficial for tasks producing forces with the fingertips during grasp (Valero-Cuevas et al., 1998). These require larger flexion torques

in the proximal joints, but smaller flexion torques at the distal joints. Such muscles require an anatomical routing that flexes the proximal joints but extends the distal joints. These muscles, in fact, exist only in the fingers and their functional anatomy is hotly debated and little understood. The interosseous or lumbrical muscles produce flexion torque at the metacarpophalangeal joint only to connect to the extensor tendons via the so-called extensor hood or mechanism. We speculate that extending the feasible torque set to span greater areas in the 4th quadrant is evolutionarily advantageous to dexterous manipulation, and that this mathematical approach can begin to explain this complex anatomical layout.

The feasible torque set also provides a context to clarify important aspects about muscle redundancy and co-contraction. Note that muscle redundancy—the ability to produce a given net joint torque with a (theoretically infinite) variety of muscle coordination patterns—is an unavoidable consequence of the need to include the origin of the torque space, even with the minimal number of $N + 1$ muscles (Fig. 5). The feasible muscle force set and the feasible torque set are convex (Chvátal, 1983) because any internal point can be reached by a linear combinations of their extreme points (vertices). These vertices are, of course, defined by positive linear combinations of the basis vectors. Muscle redundancy is simply the fact that any internal points of the feasible torque or wrench sets (i.e., a specific net joint torque or endpoint wrench) can be reached by different combinations of the basis vectors of the activation, joint torque or endpoint wrench spaces (i.e., different muscle coordination patterns). Note that as one generates torques of larger magnitudes to approach the extreme points (i.e., maximal feasible net joint torques at the boundary of the set) the amount of redundancy naturally drops until producing torques at the boundary of the feasible torque or wrench set can only be done by using unique muscle coordination patterns, i.e., maximal biomechanically feasible output can only be achieved by unique coordination patterns (for a detailed discussion see (Valero-Cuevas et al., 1998; Valero-Cuevas, 2000, 2005)). Moreover, different regions of the feasible torque space will have different degrees of redundancy: some regions can be reached by "more" linear combinations of vertices than others as different regions will necessarily allow the use of more or fewer muscles.

It is often assumed that "joint co-contraction" is a choice the nervous system makes to "stabilize joints" (a loosely used term in the literature that is seldom defined). While co-contraction will often stiffen a joint (Hogan, 1985) and one can voluntarily increase the amount of co-contraction, the feasible torque set analysis clearly shows that the vector addition of the basis vectors needed to reach certain portions of the feasible torque space requires a "reversal" along some coordinate direction (i.e., joint). That is, both coordination patterns shown in the inset in Fig. 5 require a reversal in the vertical direction (i.e., co-contraction of the second joint). The reversal along the horizontal direction (co-contraction of the first joint) is, however, optional as it occurs when all three muscles are recruited. Thus, joint co-contraction is often not an option the

nervous system makes, but a simple by-product of the anatomical routing of tendons (i.e., where moment arms define the magnitude and direction of the basis vectors in torque space) (Valero-Cuevas et al., 1998; Valero-Cuevas, 2005). Unfortunately, much of the modeling work to date that predicts and interprets "optimal" muscle coordination patterns does not take into consideration these mechanical aspects of muscle redundancy and co-contraction that are independent of issues of neural optimization of muscle actions.

Consequences to Neuromuscular Control: The Feasible Wrench Set

The feasible torque set is transformed into a feasible wrench set by the mapping of joint torques through the limb (Fig. 1 and equations 3 and 7).

$$\vec{w} = J^{-T}(\vec{q})\vec{\tau} = J^{-T}(\vec{q})\, \underbrace{R(\vec{q})\, \underbrace{F_0(\vec{q})\vec{a}}_{\vec{f}}}_{\vec{\tau}} \tag{7}$$

A similar analysis as in the preceding section can be worded in terms of the wrench basis vectors at the endpoint of the limbs and fingers. The distinct advantage of the feasible wrench set is that it shows the actual biomechanical capabilities of the musculoskeletal system in the coordinates of actual limb endpoint force and torques (Kuxhaus et al., 2005). An important computational distinction needs to be made between the calculation of the feasible wrench set and the manipulability/manipulating force ellipsoids mentioned above. The use of singular value decomposition to calculate the directions of preferential output is based on the assumption that the input to the system can be described as a unit sphere, which is valid in robotics where torque motors are used. This assumption, however, does not hold in the musculoskeletal domain where the inputs are combinations of positive basis vectors (i.e., the feasible activation set), or irregularly shaped torque capabilities (like the feasible force set). In these musculoskeletal cases one needs to use computational geometry to solve the vertex-enumeration problem for convex sets with algorithmic libraries such as qhull now in MATLAB or cdd (Avis and Fukuda, 1992; Valero-Cuevas et al., 1998). These calculations need to be repeated when the posture of the limb or finger changes because the moment arm and Jacobian matrices change nonlinearly with posture. There is also the important assumption that each basis vector can be controlled independently of the others.

The feasible wrench and torque sets effectively address the important topic of synergistic muscle action. Much research effort is being devoted to theories of "reduction of dimensionality" whereby the nervous system couples muscles so as to "simplify" their control during motor function (see for example (d'Avella and Bizzi, 2005; Tresch et al., 2006)). The reduction of dimensionality of the

controller is simply the assembly of a reduced basis of muscle vectors by coupling individual muscles into "synergies". This can be visualized in the joint torque or endpoint wrench space as simply having fewer basis vectors. Our own work has shown that the nervous system does not seem to impose such constraints on the musculature of the fingers (Valero-Cuevas et al., 1998; Valero-Cuevas, 2000, 2005), which is likely due to the disproportionately large cortical representation of finger musculature. There is always the possibility that learning of motor tasks is in essence the assembly of such coupling among muscles in both limbs and fingers. However, fixed synergies have been proposed to exist in healthy upper and lower limbs in humans and other species (d'Avella and Bizzi, 2005; Tresch et al., 2006) and are known to arise from neurological diseases such as stroke and cerebral palsy (e.g., Obholzer, 1954; Dewald et al., 1995; Mayston, 2001; Welmer et al., 2006).

The literature on muscle synergies has not explored an important consequence of reducing the number of basis vectors: the shrinking of the feasible torque and wrench sets. Adding or removing a basis vector will necessarily

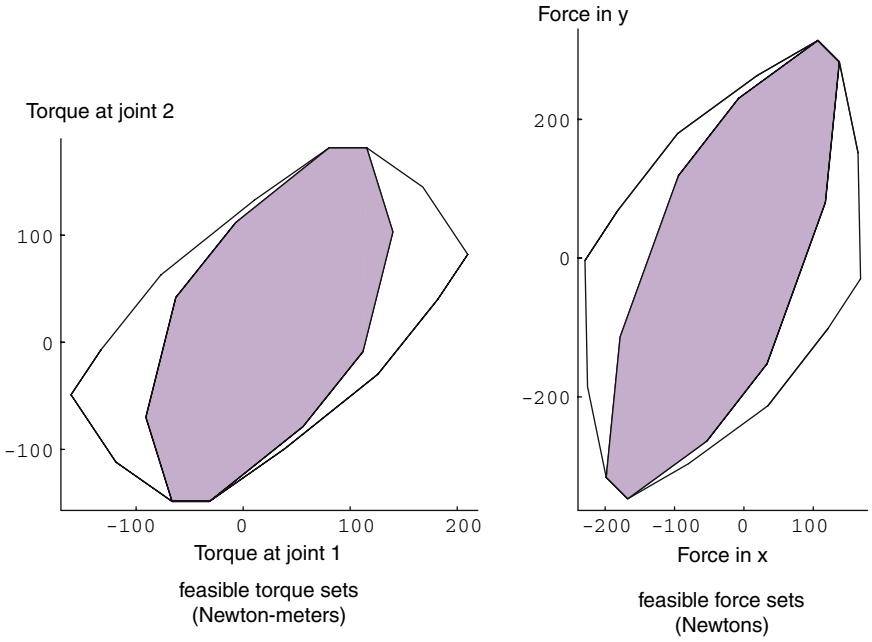

Fig. 7 Comparison of the feasible torque and feasible force sets of a system with 7 muscles that are either independently controlled (outline), or coupled by "neural synergies" (filled). The number of independently controlled actuators defines the shape and size of these feasible sets, and synergies invariably reduce the size of these sets (i.e., the feasible mechanical output). In this example, the "neural synergies" are that muscles pairs (2 and 3), and (5 and 7), must fire in unison (the 7 muscle system is not shown here for brevity). Note that there are some regions of the feasible biomechanical output that are not reachable in the presence of synergies

change the size and shape of the feasible force and wrench sets (Valero-Cuevas and Hentz, 2002; Kuxhaus et al., 2005; Valero-Cuevas, 2005). A similar effect will be obtained if, say, the basis vectors from two muscles are replaced by a single vector that represents their coupling. Thus, even if synergies could simplify the control of multiple muscles, they have the necessary consequence of reducing and changing the range of feasible mechanical output. A mathematical consequence of critical importance is that the net area of the feasible torque and wrench sets will be reduced if muscles are coupled by synergies (i.e., the boundary vertices that require independence among muscles cannot be realized) (Fig. 7). We have recorded the basis vectors for the thumb and index finger (Valero-Cuevas et al., 2000; Valero-Cuevas and Hentz, 2002; Pearlman et al., 2004) and used these changes in the feasible wrench sets to detect the functional consequences of peripheral neuropathies, both in simulation and live humans (Valero-Cuevas et al., 2000; Valero-Cuevas and Hentz, 2002; Kuxhaus et al., 2005). Thus, while the simplification of control through synergies may be advantageous in limbs used for locomotion that have more stereotypical function, there is also likely a strong evolutionary advantage to neural independence of muscle control so that the nervous system can achieve the full biomechanically feasible output of the limbs to grant them greater versatility and usefulness.

Acknowledgments This material is based upon work supported by the National Science Foundation under Grant 0237258. This publication was made possible by Grants HD048566, AR050520 and AR052345 from the NIH. Its contents are solely the responsibility of the author and do not necessarily represent the official views of the NIH.

References

Avis D, Fukuda K (1992) A pivoting algorithm for convex hulls and vertex enumeration of arrangements and polyhedra. Discrete and Computational Geometry:295–313.

Bobbert MF, van Ingen Schenau GJ (1988) Coordination in vertical jumping. J Biomech 21:249–262.

Brand P, Hollister A (1999) Clinical mechanics of the hand, 3rd Edition. St. Louis: Mosby-Year Book, Inc.

Chvátal V (1983) Linear programming. New York: W.H. Freeman and Company.

d'Avella A, Bizzi E (2005) Shared and specific muscle synergies in natural motor behaviors. Proc Natl Acad Sci U S A 102:3076–3081.

Dewald JP, Pope PS, Given JD, Buchanan TS, Rymer WZ (1995) Abnormal muscle coactivation patterns during isometric torque generation at the elbow and shoulder in hemiparetic subjects. Brain 118 (Pt 2):495–510.

Hogan N (1985) The mechanics of multi-joint posture and movement control. Biol Cybern 52:315–331.

Kuo AD, Zajac FE (1993) A biomechanical analysis of muscle strength as a limiting factor in standing posture. J Biomech 26(Suppl 1):137–150.

Kuxhaus L, Roach SS, Valero-Cuevas FJ (2005) Quantifying deficits in the 3D force capabilities of a digit caused by selective paralysis: application to the thumb with simulated low ulnar nerve palsy. J Biomech 38:725–736.

Leijnse JN (1996) A graphic analysis of the biomechanics of the massless bi-articular chain. application to the proximal bi-articular chain of the human finger. J Biomech 29:355–366.
Loeb GE (2000) Overcomplete musculature or underspecified tasks? Motor Control 4:81–83; discussion 97–116.
Mayston MJ (2001) People with cerebral palsy: effects of and perspectives for therapy. Neural Plast 8:51–69.
Obholzer A (1954) Chain-synergies in neuromuscular re-education; in the infantile cerebral flaccid-spastic syndrome. S Afr Med J 28:105–110.
Pearlman JL, Roach SS, Valero-Cuevas FJ (2004) The fundamental thumb-tip force vectors produced by the muscles of the thumb. J Orthop Res 22:306–312.
Spoor CW (1983) Balancing a force on the fingertip of a two dimensional finger model without intrinsic muscles. J Biomech 16:497–504.
Tresch MC, Cheung VC, d'Avella A (2006) Matrix factorization algorithms for the identification of muscle synergies: evaluation on simulated and experimental data sets. J Neurophysiol 95(4):2199–2212.
Valero-Cuevas FJ (2000) Predictive modulation of muscle coordination pattern magnitude scales fingertip force magnitude over the voluntary range. J Neurophysiol 83:1469–1479.
Valero-Cuevas FJ (2005) An integrative approach to the biomechanical function and neuromuscular control of the fingers. J Biomech 38:673–684.
Valero-Cuevas FJ, Hentz VR (2002) Releasing the A3 pulley and leaving flexor superficialis intact increase palmar force following the Zancolli lasso procedures to prevent claw deformity in the intrinsic minus hand. J Orthop Res 20:902–909.
Valero-Cuevas FJ, Zajac FE, Burgar CG (1998) Large index-fingertip forces are produced by subject-independent patterns of muscle excitation. J Biomech 31:693–703.
Valero-Cuevas FJ, Towles JD, Hentz VR (2000) Quantification of fingertip force reduction in the forefinger following simulated paralysis of extensor and intrinsic muscles. J Biomech 33:1601–1609.
van Ingen Schenau GJ, Bobbert MF (1993) The global design of the hindlimb in quadrupeds. Acta Anat (Basel) 146:103–108.
van Soest AJ, Schwab AL, Bobbert MF, van Ingen Schenau GJ (1993) The influence of the biarticularity of the gastrocnemius muscle on vertical-jumping achievement. J Biomech 26:1–8.
Welmer AK, Holmqvist LW, Sommerfeld DK (2006) Hemiplegic limb synergies in stroke patients. Am J Phys Med Rehabil 85:112–119.
Winter DA (1990) Biomechanics and motor control of human movement, 2nd Edition. New York: Wiley.
Yoshikawa T (1990) Foundations of robotics: analysis and control. Cambridge: The MIT Press.